

# Orbital Correlations in the Ferromagnetic Half-Metal $CrO_2$

M. S. Laad<sup>1</sup>, L. Craco<sup>2</sup> and E. Müller-Hartmann<sup>1</sup>

<sup>1</sup>*Institut für Theoretische Physik, Universität zu Köln, Zùlpicher Strasse, 50937 Köln, Germany*

<sup>2</sup>*Instituto de Física Gleb Wataghin - UNICAMP, C.P. 6165, 13083-970 Campinas - SP, Brazil*

(October 25, 2018)

We deduce a model relevant for the description of the ferromagnetic half-metal Chromium dioxide ( $CrO_2$ ), widely used in magnetic recording technology. The model describes the effect of dynamical, local orbital correlations arising from local quantum chemistry of the material. A finite temperature solution of the model in  $d = \infty$  provides a natural explanation of the optical response, photoemission, resistivity and the large Woods-Saxon ratio observed in experiments. Our study confirms the important role of many body dynamical correlation effects for a proper understanding of the metallic phase of  $CrO_2$ .

PACS numbers: 75.30.Mb, 74.80.-g, 71.55.Jv

Colossal Magnetoresistive (CMR) materials have been the focus of renewed theoretical and experimental investigations [1,2] in recent years, given their obvious technological potential. Interest has mainly been centered around the manganites, where the interesting ferromagnetic metallic regime is driven by the double-exchange (DE) mechanism, though a unified understanding of the correlated nature of the metallic state itself, as well as the high- $T$  insulating paramagnet, requires consideration of orbital correlations and the Jahn-Teller (JT) distortion on an equal footing with the DE ferromagnetism.

Some attention has also focused on  $CrO_2$ , widely used in magnetic recording tapes. In contrast to the manganites, stoichiometric  $CrO_2$  is already a ferromagnetic metal. Given the formal 4+ valence state of  $Cr$ , the two 3d electrons occupy the  $t_{2g}$  orbitals. One would intuitively expect to form  $S = 1$  spin on each site, and an antiferromagnetic Mott insulator. Why  $CrO_2$  is a ferromagnetic metal instead, has been answered by Korotin *et al* [3], who have carried out insightful (LDA + U) calculations for this material. Their main conclusions are: (i) the O 2p band(s) act, at least partially, as electron (or hole) reservoirs resulting in  $Cr$  being mixed-valent (like  $Mn$  in doped manganites), explaining metallicity, (ii) an almost dispersionless majority spin band of predominantly  $d$  character at about 1eV below  $E_F$  over a large region of the Brillouin zone. This corresponds to strongly localized  $xy$  orbitals completely occupied by one majority spin electron. On the other hand, the  $d$  states of predominantly  $d_{yz+zx}$  character hybridize with the O 2p band and disperse, crossing  $E_F$ . The Hund's rule coupling between the localized  $d_{xy}$  spin and the spin density of the band  $d_{yz+zx}$  electrons polarizes the latter, giving a ferromagnetic state via the double-exchange mechanism. Thus, both the metallicity and ferromagnetism are correlated well with each other.

A closer examination reveals that the metallic state of  $CrO_2$  is strongly correlated, implying that many-body correlation effects beyond the local-density approximation (LDA) [4] (or its variants) need to be considered.

A number of experimental observations tend to support such a picture:

(1) Polarization dependent XPS measurements reveal substantial ligand orbital polarization. An exchange splitting energy of  $\Delta_{ex-spl} \simeq 3.2$  eV was deduced [5], implying substantial correlation effects. On the other hand, LSDA calculations yield  $\Delta_{ex-spl} \simeq 1.8$ eV!

(2) The resistivity shows a behavior characteristic of correlated Fermi liquids [6]:  $\rho(T) = \rho_0 + AT^2 + BT^{7/2}$ , the last term coming from the carrier scattering of two-magnon fluctuations in a double-exchange ferromagnet [7]. A similar kind of behavior has also been observed in the CMR manganites in the FM metallic phase [7]. In fact,  $CrO_2$  falls into the “bad metal” classification, with high- $T$  ( $T > T_c^{FM} = 390$ K) resistivity exceeding the Mott limit [10]. The coefficient  $A$  is large, and in fact the ratio  $A/\gamma^2$  ( $\gamma$  is the coefficient of the linear term in the electronic specific heat) is close to the value expected for heavy-fermion metals [8], implying substantial correlation effects in the Cr  $d$ -band.

(3) Additional evidence comes from the optical conductivity data, which reveals a Drude conductivity at low energies, followed by a broad bump around 0.8eV and high-energy features centered around 3eV [9]. While the Drude part is understandable within the LSDA approach, the other features mentioned above are seen at energies that are systematically 10 – 20 percent *lower* than those predicted by the LSDA calculation, showing up the importance of correlation effects in this material [9].

(4) Additionally, recent magnetotransport measurements show interesting features. Firstly, the magnetoresistance is *linear* in fields upto 1 Tesla, and shows no evident relation with the magnetization [10]. On the other hand, it was found that the longitudinal and transverse MR is negative and increases linearly with field for  $T > 200$ K, while having a concave shape as a function of field for lower  $T$  [10], passing through minima as functions of field around  $T \simeq 200$ K. It is interesting to notice that similar behavior is also observed for manganites,  $La_{1-x}Sr_xMnO_3$  with  $x = 0.175, 0.2$  [12]. An under-

standing of the observed crossovers around  $T = 200\text{K}$  requires the consideration of additional mechanism(s) over and above the double-exchange interaction, since these features occur deep inside the ferromagnetic metallic phase ( $T_c = 390\text{K}$ ).

(5) Existing photoemission data on  $CrO_2$  show features that are more characteristic of a semiconductor with vanishing DOS at the Fermi level than of a good metal [11], completely consistent with the "bad metal" classification made in the resistivity measurements. Such features, also observed in the metallic FM state of the CMR manganites, have been linked to the strong Jahn-Teller distortions known to exist for CMR manganites [17]. However, neither the static J-T distortion, nor the doping-induced static disorder is present in  $CrO_2$ , leaving one to look for alternative scenarios to understand the suppression of low-energy spectral weight in PES.

We start by noticing that the emergence of a coherent, strongly correlated Fermi liquid scale required to understand the above features is out of reach of LDA based calculations (within which a large Woods-Saxon ratio is inexplicable, for example), as well as of calculations based on pure double exchange models. This is because these features are observed deep inside the ferromagnetic metallic state, and are thus related to additional scattering mechanisms in a half-metallic situation (where one deals with a fully spin-polarized band). In this paper, we argue that the above effects can indeed be understood by invoking the important role of strong local, orbital correlations in the  $t_{2g}$  sector (see below).

An understanding of features mentioned above should go hand-in-hand with the basic electronic structure. In this context, the LSDA+U calculation carried out by Korotin *et al.* [3] already provides the necessary ingredients to pursue more detailed investigations. The necessary ingredients seem to be: (1) Strong, local Hubbard  $U$  and Hund's rule coupling,  $J_H$ . (2) Hybridization of the  $d_{yz+zx}$  band with the  $p$  band of the  $O$ , resulting in  $Cr$  being mixed-valent, like  $Mn$  in the manganites. As pointed out in [3], the fact that  $CrO_2$  is in the class of negative charge-transfer gap materials makes this  $d-p$  hybrid band self-doped. The well known double-exchange mechanism then drives the FM metallic phase.

An examination of Figs. (3)-(4) of Ref. [4] shows that the the bands crossing the Fermi level have comparable  $d_{xz+yz}$  and  $d_{yz-zx}$  character, as well as a non-dispersive  $d_{xy}$  band centered  $1\text{eV}$  below  $\mu$ . We shall consider the  $O$  band to act solely as a reservoir of carriers, serving to make the  $d$ -band manifold non-half-filled [4]. The almost complete spin polarization tells us that the local Hund's rule coupling is strong. If this is so, we have to assume that the on-site Coulomb repulsion (the intra-orbital Hubbard  $U$ ) is stronger. Given the above, we are then led to consider a two-orbital Hubbard-like model in the double exchange (DE) limit,  $U, J_H \gg t_{a,b}$  ( $a, b$  la-

bel orbital indices). The relevant minimal model for our purpose is written as,

$$H = H_1 + H_2 \quad (1)$$

where

$$H_1 = - \sum_{\langle ij \rangle \sigma} t_{ij}^{ab} (c_{ia\sigma}^\dagger c_{jb\sigma} + h.c.) + U \sum_i (n_{ia\uparrow} n_{ia\downarrow} + a \rightarrow b) \quad (2)$$

and

$$H_2 = U_{ab} \sum_{i\sigma\sigma'} n_{ia\sigma} n_{ib\sigma'} - J_H \sum_i \mathbf{S}_i \cdot (\sigma_i^a + \sigma_i^b) \quad (3)$$

In the above, we shall assume that the effects of the actual bandstructure have been incorporated into the effective hopping strengths by fitting the idealized bandstructure to the actual one; this has been employed with much success for the cuprates [13]. We shall henceforth treat the  $t^{ab}$  as parameters of the effective model above.  $U_{ab}$  is the local, inter-orbital Coulomb repulsion,  $\mathbf{S}_i$  is the localized spin in the  $d_{xy}$  orbital, and that  $a = d_{xz+yz}$  and  $b = d_{yz-zx}$ . In the DE limit, the states corresponding to a carrier aligned antiparallel to the core-spin are projected out, and so one can drop the spin indices in the above eqn, at the price of introducing a magnetization-dependent hopping,  $t_{ij}^{ab} = t_{ij}^{ab}(\mathbf{S})$ . In this situation, the orbital index plays the role of the spin, and so one is finally left with a generalized Hubbard model in orbital space. To proceed, we will further make an assumption which does not qualitatively affect the final conclusions (see below). We will assume that the hopping matrix is diagonal in orbital space,  $t_{ij}^{ab} = t_{ij} \delta_{ab}$  [14], and choose  $t^{aa} = t_1$  and  $t^{bb} = t_2$ . Finally, we introduce new fermion operators,  $c_\uparrow = (c_a + c_b)/\sqrt{2}$ , and  $c_\downarrow = (c_a - c_b)/\sqrt{2}$ . The Hamiltonian now becomes,

$$H = - \sum_{\langle ij \rangle \sigma} t_\sigma(\mathbf{S}) (c_{i\sigma}^\dagger c_{j\sigma} + h.c.) + U \sum_i n_{i\uparrow} n_{i\downarrow} \quad (4)$$

At low- $T$  ( $< T_c^{FM} = 390\text{K}$ ), the hopping is a function of the magnetization,  $t_\sigma(\mathbf{S}) = t_\sigma(M) = t_\sigma [1 + \langle S_i^z S_j^z \rangle / 2S^2]^{1/2}$  with  $M = N^{-1} \sum_i \langle S_i^z \rangle$ , so one has to deal with a Hubbard model in orbital space with an orbital pseudo-spin and magnetization dependent hopping. In the above eqn. (4),  $t_\uparrow = (t_1 + t_2)$ , and  $t_\downarrow = (t_1 - t_2)$ . The case  $t_1 = t_2$  has been considered in [14], where the anomalous FM metallic phase of the manganites is sought to be understood in terms of the non-FL state of the effective Falicov-Kimball model in  $d = \infty$  [15]. An exact solution of the FKM in this limit reveals that the non-FL behavior is driven by a divergence in the local excitonic correlation function at low energy. In contrast, there is evidence that the FM metallic phase in  $CrO_2$  as well as in  $La_{0.7}Sr_{0.3}MnO_3$  is a correlated Fermi liquid at low  $T$ , requiring us to work with the model, eqn. (4).

In what follows, we will explain much of the observed features mentioned above in terms of the  $d = \infty$  solution of the effective Hubbard model (eqn. (4)). To understand where the local FL behavior comes from, we notice that the model, eqn. (4) with  $t_1 = t_2$ , can be mapped onto the x-ray edge problem with the recoilless local scatterer (the  $\downarrow$ -spins) right at the Fermi surface. In this case, the spectral fn. of the  $\downarrow$ -spin fermion, as well as that of the “exciton” [15] is divergent at low energy. The case  $t_1 \neq t_2$  corresponds to allowing the scatterer to recoil, killing the infrared divergence and restoring FL behavior at low  $T$  ( $T < E_R$ , the recoil energy of the  $\downarrow$ -spin [15]). In the  $d = \infty$  solution of the model, however, FL coherence sets in below the lattice coherence scale,  $T_{coh}$  (related to  $t_1 - t_2$ ).

It is instructive to summarize what is known about the Hubbard-like model, eqn. (4), in the  $d = \infty$  limit [15]. Above  $T_{coh}$ , the metallic state off half-filling is not a Fermi liquid, and the dynamics of the carriers is determined by inelastic scattering off the effectively unquenched local moments (orbital moments in our approach). Below  $T_{coh}$ , the local moments are screened by the “conduction electron” spin density, giving a Fermi liquid response. This coherence scale can be driven quite low for given  $t_1 - t_2$  resulting in an anomalous response at not too low  $T$ . In particular, the suppression of quasi-particle features in the local DOS for  $T > T_{coh}$  [16] would result in: (a) a non-Drude optical response, (b) a pseudogap feature in photoemission, (c) absence of the  $T^2$  term in the resistivity and an anomalous  $T$ -dependence of the Hall constant [16], and (d) lastly, one would expect the FL coherent response below  $T_{coh}$  to manifest itself in these responses as  $T$  is lowered. In particular, below  $T_{coh}$ , one expects a  $T^2$  component in the resistivity, a low energy Drude response in the optical conductivity, a coherent feature in the photoemission lineshape at the Fermi surface, and a  $T$ -independent normal Hall constant (the anomalous Hall effect requires more work [18]).

Given that the para-orbital metallic state of the above model with  $t_1 \neq t_2$  is a correlated Fermi liquid, one expects perturbations like disorder to tilt the balance in favor of low-energy incoherence. In particular, with modest disorder [19], the incoherent metallic state gives rise to an incoherent lineshape in PES and a pseudogapped behavior in the optical response, even at low- $T$ .

With this information in mind, we are ready to discuss our results. In our calculations, we have employed a gaussian unperturbed DOS, and two values of temperature:  $T = 0.01D$  and  $T = 0.1D$  ( $D$  is the half-width of the gaussian). We have chosen  $U_{ab} = 3D_{\uparrow}$ , where  $D_{\uparrow}$  is the effective  $\uparrow$ -spin bandwidth, and the bandfilling,  $n = n_{\uparrow} + n_{\downarrow} = 0.8$ . In the  $d = \infty$  approximation that we use,  $t_{\sigma}(M) = t_{\sigma}[(1 + M^2(T))/2]^{1/2}$  with  $M(T)$  taken from the spherical model limit for the Heisenberg model.

In  $d = \infty$ , all relevant information about the local dynamical fluctuations is encoded in a purely local irre-

ducible self-energy,  $\Sigma(\omega)$ , entering the lattice Green function for the model under consideration:

$$G(k, \omega) = G(\epsilon_k, \omega) = \frac{1}{\omega + \mu - \epsilon_k - \Sigma(\omega)} \quad (5)$$

To solve the model in  $d = \infty$  requires a reliable way to solve the single impurity Anderson model (SIAM) embedded in a dynamical bath described by the hybridization fn.  $\Delta(\omega)$ . There is an additional condition that completes the selfconsistency:

$$\int d\epsilon G(\epsilon, \omega) \rho_0(\epsilon) = \frac{1}{\omega + \mu - \Delta(\omega) - \Sigma(\omega)} \quad (6)$$

where  $\rho_0(\epsilon)$  is the free DOS ( $U = 0$ ). The above eqns. (4)-(6) refer to the disorder-free Hubbard model. In  $d = \infty$ , this is sufficient to compute the transport, because the vertex corrections in the Bethe Salpeter eqn. for the conductivity vanish identically in this limit [15]. Thus, the conductivity is fully determined by the basic bubble diagram made up of fully interacting local GFs of the lattice model.

The optical conductivity is computable in terms of the full  $d = \infty$  GFs as follows [15]:

$$\sigma_{xx}(i\omega) = \frac{1}{i\omega} \int d\epsilon \rho_0(\epsilon) \sum_{i\nu} G(\epsilon, i\nu) G(\epsilon, i\nu + i\omega) \quad (7)$$

and the dc resistivity is just  $\rho_{dc}(T) = 1/\sigma_{xx}(0, T)$ .

To solve the impurity model, we have used the iterated perturbation theory adapted to our model. We use the IPT because it is analytic in  $U$  and yields results in good agreement with exact diagonalization studies [15]. In view of the ability of the IPT to reproduce all the qualitative aspects observed in  $\sigma_{xx}(\omega)$ , we believe that is a good tool in the present case. We mention that we have extended the IPT off half-filling to finite temperatures (as far as we are aware, such an undertaking has not been carried out earlier). We have checked that our results agree fully with those obtained by others at  $T = 0$ .

The photoemission lineshape is given simply by,

$$I_{PES}(\omega) = \rho(\omega - \mu, T) f(\omega - \mu) \quad (8)$$

where  $f(\omega) = (e^{\omega/T} + 1)^{-1}$  is the Fermi fn.

To make closer contact with experiment, we notice that, in  $CrO_2$ ,  $Cr$  exists in two crystallographically inequivalent sites, resulting from a particular kind of orbital ordering [3]. The potential fluctuation arising from this is of order of the crystal field splitting ( $\simeq 1 - 1.5$  eV), providing an intrinsic source of disorder scattering (especially at  $T \simeq 300K$  at which the PES experiment was performed), further reducing the coherent spectral weight at  $\mu$ . Hence, we have considered the effects of scattering off an additional local, static and random potential  $v = U/4$ , assuming a binary distribution,  $P(v_i) = [\delta(v_i) + \delta(v_i - v)]/2$  (an additional assumption

is that the material is composed of an equal composition of the two inequivalent sites). To this purpose we have used the IPT (for correlations) in combination with the CPA for disorder, in a selfconsistent way [19].

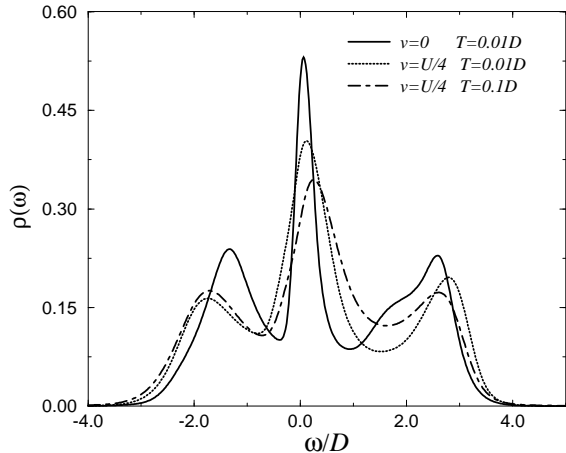


FIG. 1. The density of states (DOS) for  $U/D = 3.0$ ,  $\delta = 0.2$ ,  $T = 0.01D$  and two values of local disorder potential:  $v = 0$  (continuous) and  $v = U/4$  (dotted line). The dot-dashed line is the DOS for the same parameters as above and  $v = U/4$  but with  $T = 0.1D$ .

In Fig. 1, we show the local spectral density,  $\rho(\omega)$  for our model at different  $T$  for  $U/D = 3.0$ . This ratio was chosen because we are interested in dealing with the metallic phase here. It is clearly seen that the collective “Kondo” resonance is strongly  $T$  dependent because of particle-hole pair generation; above  $T \simeq T_{coh} = 0.13$ , the coherent feature is completely washed out, and the physics is understood in terms of carriers scattered inelastically off effectively unquenched *orbital* moments, in analogy with the situation in the usual Hubbard model. This has important consequences for the optical and spectroscopic response, as we describe below.

At low  $T$ , the optical conductivity shows a sharp Drude peak characteristic of a correlated FL metal. This peak carries a small part of the total spectral weight, and most of it is distributed over a wide energy scale of  $3eV$ , comprising the rather well pronounced mid-IR absorption and higher energy features (Fig. 2). Increasing  $T$  ( $T = 0.1D$ ), we see that the Drude weight is reduced and the higher energy features are smoothed out, again resembling qualitatively the situation in  $CrO_2$  [9].

The d.c resistivity (not shown) is computed from the  $\omega = 0$  part of the optical conductivity, and clearly exhibits the quadratic behavior in  $T$ :

$$\rho_{dc}(T) \simeq \tau^{-1}(T) = \pi^2(U^2/D^3)n/2(1 - n/2)T^2 \quad (9)$$

With an effective mass enhancement of approximately 3 for  $U_{ab}/D = 3.0$ ,  $n = 1.3 \cdot 10^{28} m^{-3}$ ,  $\rho(\mu) = 0.55 eV^{-1}$  and

$n = 0.8$ , we obtain  $A/\gamma^2 \simeq 4 - 5 \cdot 10^{-5}$ , as reported in Ref. [8].

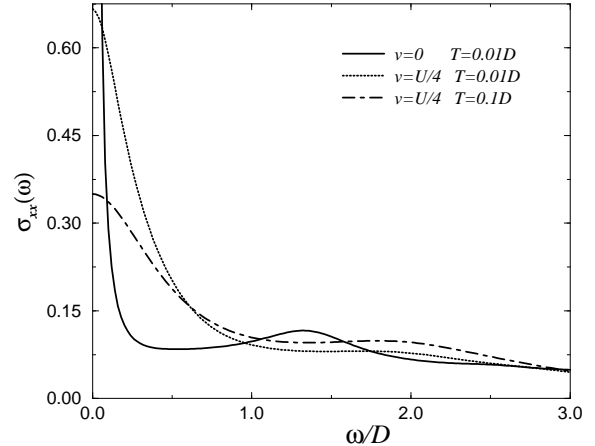


FIG. 2. Real part of the optical conductivity  $\sigma_{xx}$  for  $U/D = 3.0$ ,  $\delta = 0.2$   $v = 0$  (continuous) and  $v = U/4$  (dotted), all at  $T = 0.01D$ . The dot-dashed line shows  $\sigma_{xx}$  for  $U/D = 3.0$ ,  $\delta = 0.2$ ,  $v = U/4$  and  $T = 0.1D$ . The computed result shows all the features observed in Ref. [9].

Next we turn to angle integrated photoemission, which measures the occupied part of the single-particle DOS, in Fig. 3. As expected from the  $T$ -variation of the DOS, we see a sharp Fermi step at  $T = 0.01D$ , a reduced step feature at  $T = 0.1D$ , and completely incoherent response in the pseudogap phase. A comparison of the results with those observed experimentally shows that the calculated spectral weight at the Fermi surface ( $\omega = 0$ ) is quite

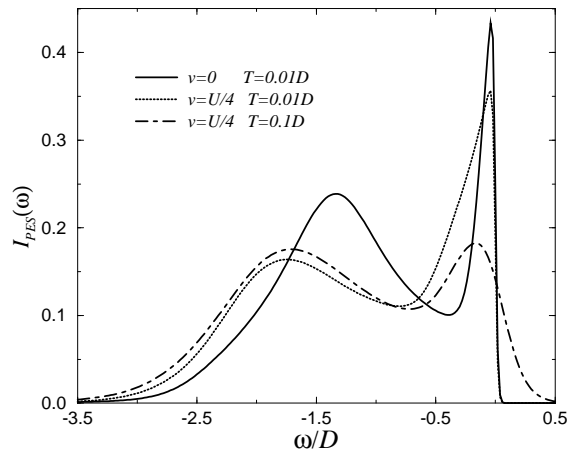


FIG. 3. The integrated photoemission lineshapes for our model with  $U/D = 3.0$ ,  $\delta = 0.2$  and for two values of the disorder strength  $v$  and the temperature  $T$ . Introduction of disorder brings the lineshape much closer to that observed experimentally by moving low energy spectral weight to higher energy.

small, but still finite, while *complete* depletion of the low energy spectral weight is observed experimentally. The almost complete depletion of the low-energy spectral weight observed experimentally is then interpreted in terms of the  $T$ -dependence of the local spectral density. If the temperature of measurement is higher than the lattice coherence scale, the FL-like feature is washed out, reducing the spectral weight at  $\mu$ , and making the intensity resemble that of a semiconductor. In this context, we would like to mention that the PES experiment was carried out at  $T = 300$  K, which is pretty high. The calculation carried out above does yield an incoherent response at  $T = 0.1D$  and the spectral weight at  $\mu$  is quite small but is still non-vanishing at  $\mu$ .

As we have mentioned before, the results for a moderate disorder  $v = U/4$  resemble experimental observations more closely (fig. 3). However, it may also be the case that short-ranged orbital correlations enhance the tendency to open up a pseudogap, reducing the DOS beyond that found in the  $d = \infty$  calculation. At this moment, this discrepancy between theory and experiment remains unclear. A more precise undertaking should also include the real bandstructure of  $CrO_2$ ; in this context, we notice that the LDA calculations already yield a dip in the DOS at  $E_F$  [3]. We are of the opinion that the real situation involves a combination of all the above factors, and plan to address these in a future publication. We suggest that more information concerning the  $T$ -dependence of the low-energy spectral weight, could be obtained from a simultaneous study of optical and PES spectra taken at different temperatures across the ferro-para transition. This could be used to discriminate between different scenarios proposed for  $CrO_2$ . If the ideas proposed here are correct, one expects a  $T$ -dependent build-up of coherent spectral weight at low energy as  $T$  is lowered through the para-ferro transition.

Finally, we observe that the model hamiltonian proposed in this paper can explain the orbital polarization observed by Stagaescu *et al.* [5]. Indeed, for a generic choice of the  $t_\alpha, \alpha = 1, 2$ , with  $t_1 \neq t_2$ , an orbital polarization is spontaneously generated in our model. A complete analysis of these effects requires consideration of actual bandstructure within the  $d = \infty$  approximation that we've used here, and we plan to treat this issue in the future.

In conclusion, we have shown, based on the LDA+U results of Korotin *et al.* [3], how the various observed "strongly correlated" properties of the half-metallic ferromagnet  $CrO_2$  can be understood by invoking the role of dynamical orbital correlations and Hund's rule double exchange in the  $t_{2g}$  sector. The treatment presented here should also be valid for other transition metal based half-metallic ferromagnets [2]. Our results are consistent with the view that LSDA calculations [3] need to be supplemented by treatments including dynamical correlation effects to understand the physics of  $CrO_2$ .

## ACKNOWLEDGMENTS

MSL acknowledges the financial support of the Sfb341 of the German DPG. LC was supported by the Fundação de Amparo à Pesquisa do Estado de São Paulo (FAPESP).

- 
- [1] for a review, see, for example, *Colossal Magnetoresistive Oxides*, ed. Y. Tokura (Gordon and Breach) in press.
  - [2] M. Imada, cond-mat/0004232.
  - [3] M. Korotin *et al.*, Phys. Rev. Lett. **80**, 4305 (1998). I also thank Prof. Sawatzky for correspondence related to the additional scattering arising from a particular kind of orbital ordering found in their calculation.
  - [4] I. Mazin, D. J. Singh and C. Ambrosch-Draxl, Phys. Rev. B **59**, 411 (1999).
  - [5] A. Stagaescu, *et al.*, cond-mat 9910346, to be published in Phys. Rev. B.
  - [6] L. Ranno, A. Barry and J. M. D. Coey, J. Appl. Phys. **81**, (8), 5774 (1997).
  - [7] V. Yu. Irkhin and M. Katsnelson, Phys. Usp. **37**, 659 (1994).
  - [8] K. Suzuki and P. Tedrow, Phys. Rev. B **58**, 17, 11597 (1998).
  - [9] D. Basov, *et al.*, Phys. Rev. B **60**, 4126 (1999).
  - [10] see ref.[8]; also A. Barry, Ph.D thesis, University of Dublin, unpublished.
  - [11] K. Kämper *et al.*, Phys. Rev. Lett. **59**, 2788 (1987).
  - [12] A. Ramirez, J. Phys. Condens. Matter. **9**, 8171 (1997).
  - [13] see E. Stechel, in *High Temperature Superconductivity*, eds. B. Coffey *et al.*, (Addison-Wesley, 1989).
  - [14] the actual situation is a bit more complicated than what we have assumed here, but in the ferromagnetic metallic state, we expect the qualitative features to remain unchanged. See, for example, V. Ferrari, *et al.*, cond-mat/9906131.
  - [15] A. Georges *et al.*, Revs. Mod. Phys. **68**, 13 (1996).
  - [16] P. Majumdar and H. R. Krishnamurthy, cond-mat 9512151.
  - [17] see, for example, A. J. Millis, P. B. Littlewood and B. I. Shraiman, Phys. Rev. Lett. **74**, 5144 (1995).
  - [18] F. E. Maranzana, Phys. Rev. **160**, 421 (1967).
  - [19] M. S. Laad, L. Craco and E. Müller-Hartmann, cond-mat/9911378, submitted to Phys. Rev. B.